Orbital and magnetic orderings in localized t_{2g} systems, YTiO$_3$ and YVO$_3$: Comparison with a more itinerant e_g system LaMnO$_3$

H. Sawada*

Joint Research Center for Atom Technology, Angstrom Technology Partnership, 1-1-4 Higashi, Tsukuba, Ibaraki 305, Japan

K. Terakura

Joint Research Center for Atom Technology, National Institute for Advanced Interdisciplinary Research, 1-1-4 Higashi, Tsukuba, Ibaraki 305, Japan
and Institute of Industrial Science, University of Tokyo, 7-22-1 Roppongi, Minato-ku, Tokyo 106, Japan

The electronic structures of the narrow t_{2g} band systems YTiO$_3$ and YVO$_3$ are studied using the generalized gradient approximation (GGA) and local-density approximation (LDA)+U method. GGA fails in reproducing the insulating nature of YTiO$_3$ and the correct magnetic ordering of YVO$_3$. The LDA+U method improves the GGA results in both of the above contexts through the enhancement in the orbital polarization. These results are compared with those for the wider t_{2g} band system LaVO$_3$ and more itinerant e_g system LaMnO$_3$. The problems of GGA and LDA+U in predicting the ground-state magnetic ordering of LaMnO$_3$ will also be discussed. [S0163-1829(98)07332-9]

I. INTRODUCTION

In a previous series of papers,[1–6] we studied basic aspects of the transition-metal oxides (TMO) with the perovskite structure based on the band structure calculations. Particular attention has been paid to the correlation among lattice distortion, orbital ordering, and magnetic ordering. We adopted the local-spin-density approximation (LSDA), the generalized gradient approximation[7,8] (GGA) and the local-density approximation (LDA)+U method[9,10] as different levels of approximations to treat the electron-electron interaction. The perovskite TMO are categorized into two groups, the t_{2g} system and the e_g system, where the Fermi level is located in the t_{2g} and e_g manifold, respectively. While the e_g orbitals are more or less itinerant because of the strong hybridization with the oxygen p orbitals, the t_{2g} orbitals have much stronger localized character due to the weak p-d hybridization. With given crystal structures determined experimentally, the calculated degree of orbital polarization is nearly the same between LSDA and GGA for the e_g system LaMnO$_3$. On the other hand, for the t_{2g} systems (LaVO$_3$, YVO$_3$, YTiO$_3$), the orbital polarization is virtually nonexisting with LSDA and becomes appreciable with GGA.[4,11] These results seem to suggest that the controlling factor of the orbital polarization may be the Jahn-Teller (JT) lattice distortion for the e_g system and the electron-electron interaction for the t_{2g} system. The total energy calculations based on GGA can correctly give the lowest energy to the observed ground-state magnetic ordering in most cases we studied. However, there were two obvious problems in our study. First, we found that the ferromagnetic (FM) state becomes more stable than the observed A-type antiferromagnetic (AF) state in LaMnO$_3$ if we optimize the JT distortion for the FM and A-type AF state separately even with experimental lattice constants for the A-type AF state.[6] The energy of the FM state decreases further with optimization of

the lattice constants. The LDA+U method with the effective Coulomb parameter U_{eff} common to both t_{2g} and e_g states even worsens the situation.[6] The reason for this is that the AF coupling contributed by the t_{2g} states is suppressed by the enhanced energy splitting between the occupied and unoccupied t_{2g} states. Second, even if we use the experimental lattice structure, the energy ordering estimated by GGA among different magnetic structures is totally incorrect for YVO$_3$, though GGA improves the LSDA result to some extent.[4,12] The failure of the GGA calculation in this case may be due to the very narrow d bands caused by the reduced angle $\angle$V-O-V [144° in YVO$_3$ (Ref. 13) versus 156° in LaVO$_3$ (Ref. 14)]. (Note that the ionic radii of Y^{3+} and La^{3+} with coordination number of 12 are 1.25 and 1.36 Å, respectively.)

In the present work we study these systems, YTiO$_3$, YVO$_3$, and LaMnO$_3$. Our previous calculation for YTiO$_3$ showed that although GGA can reproduce the magnetic order and orbital order qualitatively, it cannot reproduce the insulating nature.[11] In fact, YTiO$_3$ is an FM Mott insulator, a rare case. Note that LaTiO$_3$ is an AF Mott insulator. Mizokawa and Fujimori pointed out that the spin-orbit interaction plays an important role in LaTiO$_3$.[15] We neglect it in our study of Y compounds expecting that a larger crystal distortion in the Y case makes the crystal field more important than the spin-orbit interaction. Nevertheless, a possibility of an important role of the spin-orbit interaction will be pointed out in the intermediate temperature phase of YVO$_3$. We will show below that the LDA+U method with U_{eff} of $2\sim3$ eV resolves the problems in YTiO$_3$ and YVO$_3$. These values of U_{eff} are consistent with our previous estimation by the LDA+U$_2$ method in which the Coulomb interaction between t_{2g} electrons are allowed to be screened by the e_g electrons.[5] In the present work, we applied the same U_{eff} both to t_{2g} and e_g states but the e_g states are anyway empty.

For LaMnO$_3$, problems are rather complex. As already

TABLE I. Crystal structures and magnetic properties of $YTiO_3$ (Refs. 19–21), YVO_3 (Ref. 13), and $LaVO_3$ (Refs. 14, 22, and 23). a, b, and c are lattice constants in Å, M-O denotes the bond distance in Å between the transition metal (M) and oxygen, and $\angle$M-O-M is the bond angle in degree. M.O. denotes the magnetic order and M the magnetic moment in μ_B. T_N and T_C are Néel and Curie temperature, respectively.

| | $YTiO_3$ | YVO_3 | | $LaVO_3$ |
		$T < 77$ K	$T > 77$ K	
a (Å)	5.316	5.279	5.272	5.592
b	5.679	5.589	5.620	5.562
c	7.611	7.548	7.542	7.752
M-O (Å)	2.02	1.98	1.98	1.98, 1.98
	2.02	1.98	2.01	1.98, 1.99
	2.08	2.05	2.02	2.04, 2.04
$\angle$M-O-M (°)	140	145	144	157
	144	144	145	158, 156
M.O.	F	G	C	C
M (μ_B)	0.84	1.6	1.0	1.3
T_N or T_C (K)	29	77	118	140

mentioned, we know at least one possible reason for the failure of the LDA+U method. Therefore, just as an attempt we apply U_{eff} only to the e_g states and show that this prescription significantly improves the situation. With the LDA+U_2 method,[5] we demonstrated that the effective Coulomb interaction between t_{2g} electrons in $LaMnO_3$ is vanishingly small by the efficient screening by the e_g states. Perhaps this argument can be a rationale for the neglect of U_{eff} for the t_{2g} states. Nevertheless, the present purely empirical prescription requires justification with a more fundamental approach.

The details of the computational method are described elsewhere,[6] and here we only mention two aspects. First, the number of **k** points is 144 in the first Brillouin zone, which corresponds to 48, 56, 60, and 56 **k** points in the irreducible Brillouin zone for the FM, A-type, C-type, and G-type AF orderings, respectively. Second, the LDA+U method in the present calculations is the one implemented in the Vanderbilt pseudopotential framework with the plane-wave basis set.[16,17] Note that U and J are simply parameters and $U_{eff} = U - J$ is set to be 3.2 eV and 2.8 eV for $YTiO_3$ and YVO_3, respectively. These values of U_{eff}, which are applied to both t_{2g} and e_g electrons, give reasonable band gaps.[18]

TABLE II. The total energies (E_T)(meV/f.u.) measured from the experimentally obtained one and magnetic moments (M) (μ_B) of various spin orderings.

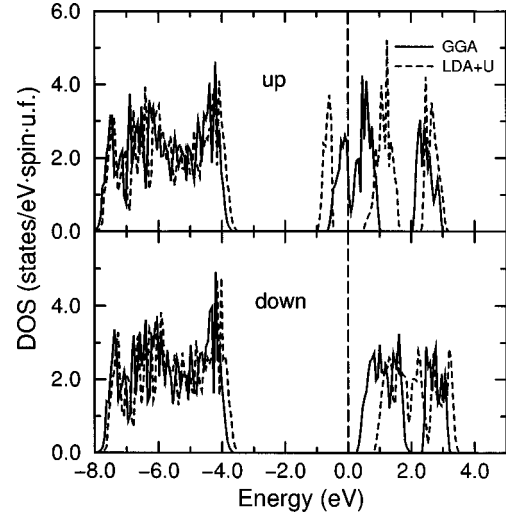| | $YTiO_3$ | | | | YVO_3 | | | |
| | GGA | | LDA+U | | GGA | | LDA+U | |
	E_T	M	E_T	M	E_T	M	E_T	M
FM	0.0	0.80	0.0	0.82	−67.4	1.76	48.3	1.81
A-type AF	8.1	0.71	2.0	0.81	−45.7	1.69	33.8	1.78
C-type AF	54.5	0.19	9.8	0.77	−41.8	1.61	15.6	1.77
G-type AF	37.0	0.23	10.5	0.76	0.0	1.56	0.0	1.73

FIG. 1. Comparison of the total DOS for $YTiO_3$ obtained in GGA and LDA+U.

II. RESULTS AND DISCUSSION

Table I summarizes the experimental information about the crystal structures and the magnetic properties of $YTiO_3$, YVO_3, and $LaVO_3$. The most important feature to be noticed is the large deviation from 180 ° for the angles $\angle$Ti-O-Ti and $\angle$V-O-V for the Y case. It is also interesting to note the change in the V-O bond length distribution in YVO_3 associated with the change in the magnetic ordering. Table II shows the total energies of $YTiO_3$ and YVO_3 for different magnetic structures, namely, ferromagnetic (FM), A-type antiferromagnetic (AF), C-type AF, and G-type AF structures, obtained in GGA and LDA+U. In these calculations, the experimental crystal structure for the ground state magnetic order is assumed. As for $YTiO_3$, the FM state is the most stable both in GGA and LDA+U, being consistent with the experimental observation. However, the energy dif-
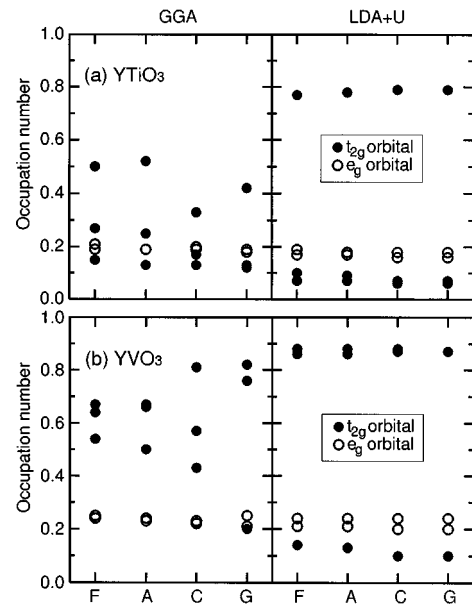

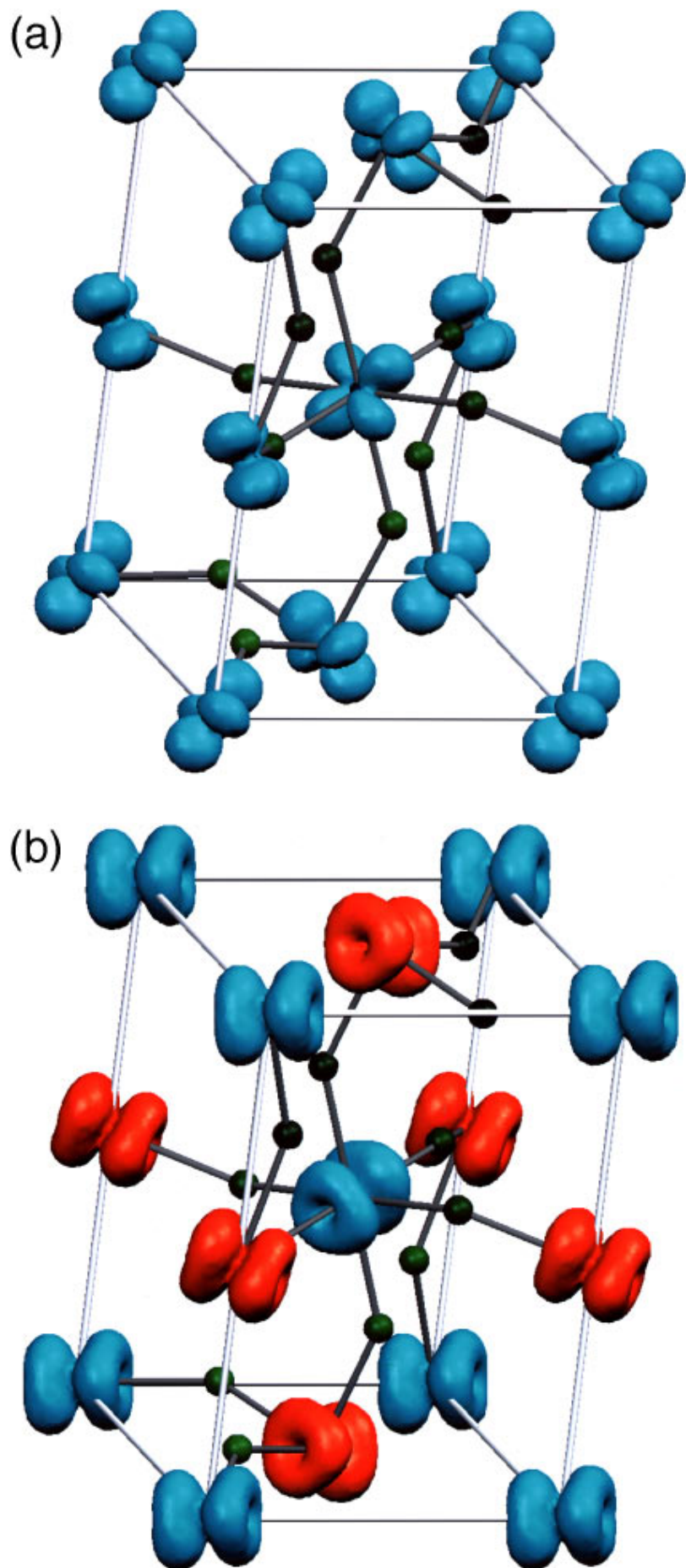FIG. 2. The orbital population in the majority spin d-states for (a) $YTiO_3$ and (b) YVO_3.

(a)

(b)

FIG. 3. (Color) The spatial d electron distribution in (a) FM YTiO$_3$ and (b) G-type AF YVO$_3$. The colors denote up-spin (blue) and down-spin (red) contributions.

ference among these magnetic structures may be too large in GGA to account for the low Curie temperature of 29 K. The LDA+U method suppresses the energy difference by about factor four. The neutron diffraction experiment for YVO$_3$ (Ref. 13) shows that the G-type AF state is the lowest-energy phase. The first-order phase transition at 77 K from the G-type to the C-type AF state suggests that the second lowest energy phase may be of the C-type AF state. Table II clearly shows that the ordering of the stability among different magnetic structures is totally incorrect in the results obtained by GGA. On the other hand, the LDA+U method resolves this problem of GGA. In the following we will analyze the origins of the difference between the GGA and LDA+U calculations for both YTiO$_3$ and YVO$_3$ by examining the density of states (DOS) and the orbital population.

The total DOS for the FM YTiO$_3$ is shown in Fig. 1 for both GGA and LDA+U. In contrast to the LSDA result shown in Ref. 11, the GGA result has a clear dip in DOS at the Fermi level. The LDA+U method produces a well-defined band gap being consistent with the experiment. The magnetic moment of Ti within a sphere of 1.16 Å is also shown in Table II. Although LDA+U gives a slightly larger value for the magnetic moment than GGA for the FM state, both are in fair agreement with the experimental value in Table I. However, the magnitude of magnetic moment of Ti strongly depends on the magnetic structure in the GGA results. The trend observed in Table II is such that the magnetic moment shrinks as the number of antiparallel pairs increases. This is because in the AF ordering the majority spin state on a given site can hybridize with the minority spin state on the neighboring site with antiparallel magnetic moment and this hybridization is strong in the Ti case due to small exchange splitting in GGA. Such hybridization reduces the magnitude of the magnetic moment. In the LDA+U calculation, the exchange splitting is significantly enhanced and thereby the intersite majority-minority hybridization is reduced. This explains the reduction not only in the variation of the magnetic moment among different magnetic orderings but also in the variation of the total energies. The latter can be associated with reduction in the kinetic exchange coupling that is roughly proportional to t^2/Δ_{ex} with t the effective $d-d$ hopping integral between neighboring Ti atoms and Δ_{ex} the exchange splitting. The orbital population in the majority spin d states are shown in Fig. 2(a). Clearly, LDA+U enhances significantly the orbital polarization. In GGA, the orbital polarization also depends on the magnetic ordering sensitively, and the small orbital population in the majority spin state for the C- and G-type AF states is due to the small magnetic moment. The total d electron number does not depend on the magnetic ordering. The spatial d-electron distribution as a result of the orbital polarization in the FM state obtained by LDA+U is shown in Fig. 3(a). As suggested by Fig. 2(a), only one t_{2g} orbital is occupied at each Ti site. An interestng feature of Fig. 3(a) is that the orbital ordering is of G-type, which is required in order to stabilize the FM state as suggested by the consideration using the diagrams like Figs. 15–17 in Ref. 4. As the crystal structure is available only above the Curie temperature,[19] the bond arrangement in the crystal structure used in our calculation is of C-type, being inconsistent with the orbital ordering. This clearly suggests that the orbital ordering is con-
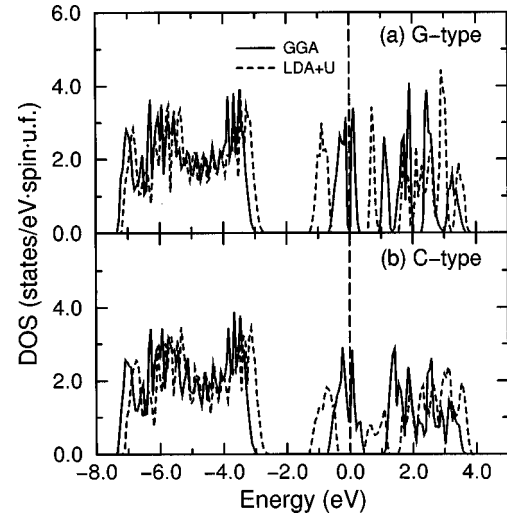

FIG. 4. Comparison of the total DOS for (a) G-type and (b) C-type AF YVO$_3$ obtained in GGA and LDA+U.

trolled by the electron correlation rather than by the electron-phonon interaction in the t_{2g} systems.

YVO$_3$ has a small band gap at the Fermi level in the G-type AF state as shown in Fig. 4(a), but it becomes metallic with other magnetic orderings in GGA. However, the band gap does not control the energetics significantly in the present case. In contrast to this, the variation in the majority spin t_{2g} bandwidth, estimated in GGA as 1.85 eV (FM), 1.52 eV (A-AF), 1.21 eV (C-AF) and 1.05 eV (G-AF), correlates with the variation in the total energies. A larger t_{2g} bandwidth results in a larger gain in the band energy. Anyway, as shown in Table II, the total energy calculations by GGA are totally incorrect for YVO$_3$. Experimentally, YVO$_3$ is an insulator with an energy gap of 1.2 eV, which is comparable to the t_{2g} bandwidth obtained by GGA. This suggests that YVO$_3$ is a strongly correlated Mott insulator and GGA fails in describing its electronic structure. The situation should be compared with that of LaVO$_3$ where GGA can predict the ground-state magnetic ordering correctly at least with the given experimental crystal structure. The difference between these two systems comes from the difference mostly in the ionic radius between La^{3+}(1.36Å) and Y^{3+}(1.25Å). The smaller ionic radius of Y^{3+} causes a smaller $\angle$ V-O-V and thereby a smaller t_{2g} bandwidth. LaVO$_3$ and YVO$_3$ form good instructive examples showing how GGA fails as the bandwidth becomes narrower.

The correct energy ordering among different magnetic structures is obtained by the LDA+U method at least with the given experimental crystal structure corresponding to the G-type AF state. The corresponding DOS is shown in Fig. 4(a) by broken curves. The calculated magnetic moment is slightly overestimated compared with the experimental value. The orbital population among the majority-spin d orbitals is shown in Fig. 2(b) for different magnetic orderings and for both GGA and LDA+U. Again, the orbital population depends strongly on the magnetic ordering in GGA, while it is quite insensitive to the magnetic ordering in LDA+U. The failure of GGA and success of LDA+U in the prediction of the ground-state magnetic ordering can be understood by the diagram of Fig. 15 in Ref. 4 with the orbital population shown in Fig. 2(b). The diagram tells us that the

AF coupling between the neighboring V moments along the *c* axis will be stabilized if the orbital polarization is strong. The condition is satisfied by the orbital polarization obtained by LDA+U but not by the one obtained by GGA as can be seen in Fig. 2(b) for the FM state. The spatial *d*-electron distribution as a result of the orbital polarization in the *G*-type AF state calculated by LDA+U is shown in Fig. 3(b). Clearly the orbital ordering is of *C*-type, the same as the bond arrangement in this case. If the local *x* axis is taken along the longest V-O bond, the electron density distribution in Fig. 3(b) corresponds to the nearly equal occupation of *xy* and *zx* orbitals.

As mentioned already, YVO$_3$ undergoes the first-order phase transition from the *G*-type to the *C*-type AF state at 77 K. An important difference in the crystal structure between the two phases is the fact that one longer V-O bond lies in the *ab* plane in the low-temperature phase while there are two longer V-O bonds in the *ab* plane in the high-temperature phase. Judging from this V-O bond-length distribution for the *C*-type AF state in Table I, we speculate that the *xy* orbital will be most preferentially occupied and the *yz* and *zx* orbitals will be both half filled in the majority spin state. With the above orbital population, an argument based on a diagram similar to Fig. 15 in Ref. 4 predicts a FM coupling between V magnetic moments along the *c* axis. On the other hand, a diagram similar to Fig. 17 in Ref. 4 suggests that the magnetic coupling within the *ab* plane may be little affected by the small rearrangement of the orbital polarization associated with the phase transition. Therefore, the bond arrangement above 77 K is favorable to the magnetic ordering of the *C*-type AF. However, the present total-energy calculation is not totally consistent with the above speculation. The *G*-type AF is still slightly lower in energy than the *C*-type AF even with the crystal structure for the *C*-type AF. The energy difference is, however, only 5 meV per formula unit, being $\frac{1}{3}$ of the energy difference shown in Table II where the total energies for YVO$_3$ were estimated for the structure for the *G*-type AF. There are two possible ingredients to be considered in the arguments on the transition from the *G*-type to *C*-type AF. First, considering the near degeneracy between *yz* and *zx* orbitals with the structure for the *C*-type AF, we expect an important role of the spin-orbit interaction. In fact, the spin-orbit coupling energy is the order of 10 meV. Second, the transition from the *G*-type to *C*-type AF may be partly caused by the entropy gain in the *C*-type AF, which we have not estimated. In Fig. 4 the DOS for the *C*-type AF shows wider V *d* band than that for *G*-type AF, reflecting the FM ordering along the *c* axis in the *C*-type AF.

Finally, we would like to make two brief comments on LaMnO$_3$. First, we have demonstrated so far that the electronic structures of the t_{2g} system like YTiO$_3$ and YVO$_3$ are significantly modified by the approximations used for the electron-electron interaction. However, the basic features of the electronic structure of LaMnO$_3$, a typical example of the e_g system, are fairly insensitive to the approximations. We demonstrated this in our previous paper[3] in detail, and here we only show in Fig. 5 the orbital population estimated by some different approximations. It is clear that the orbital population is hardly affected by different approximations and
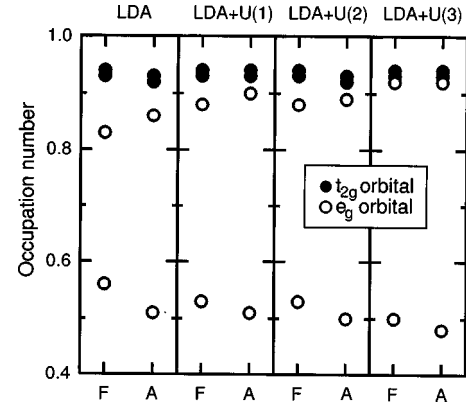

FIG. 5. The orbital population in the majority spin *d*-states for LaMnO$_3$. In LDA+U(1), U_{eff} of 2 eV is applied to the t_{2g} and e_g electrons. In LDA+U(2) and LDA+U(3), U_{eff} of 2 eV and 4 eV is applied only to the e_g electrons, respectively.

different parameter values in LDA+U. Second, we pointed out in the Introduction one serious problem of our band structure calculation for LaMnO$_3$: if we optimize the crystal structure, the FM state rather than the *A*-type AF state becomes the ground state. As long as we use the common U_{eff} for both t_{2g} and e_g orbitals in the LDA+U method, the situation is never improved or even becomes worse than GGA calculations. If we adopt the orbital dependent U_{eff} and solve the LDA+U equations within the Hartree-Fock approximation, one of the possible ways to make the *A*-type AF more stable is to apply U_{eff} only to the e_g orbitals. This seems to contradict with the expectation that the e_g states are more itinerant than the t_{2g} states. However, in the LDA+U$_2$ approach[3] developed by us where the electron-electron interaction in the t_{2g} orbitals is allowed to be screened by the e_g electrons, the screened U_{eff} for the t_{2g} orbitals is vanishingly small in LaMnO$_3$ because of very efficient screening by the e_g states located just at the Fermi level. However, a problem is that any hint about U_{eff} for the e_g orbitals is not given by the LDA+U$_2$ method. The efficient screening of the t_{2g} electrons by e_g electrons in LaMnO$_3$ will be a real fact irrespective of the approaches. Therefore, just as an attempt, we apply U_{eff} only to the e_g orbitals. Figure 6 shows the energy
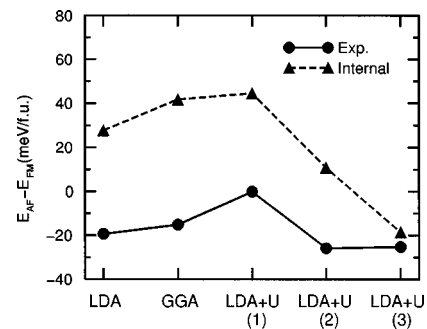

FIG. 6. The energy difference between *A*-type AF and FM states for LaMnO$_3$ estimated by some different approximations. The experimental crystal structure was used for circles. For triangles the internal coordinates are optimized with the experimental lattice parameters. In LDA+U(1), U_{eff} of 2 eV is applied to the t_{2g} and e_g electrons. In LDA+U(2) and LDA+U(3), U_{eff} of 2 eV and 4 eV is applied only to the e_g electrons, respectively.

difference between the A-type AF and FM states estimated by some different approximations. For circles we used the crystal structure obtained experimentally. For triangles we optimized the internal coordinates with the experimental lattice parameters for the A-type AF state. It is clear that after the internal coordinate optimization the LDA+U method with U_{eff} only to the e_g orbitals can stabilize the A-type AF. Nevertheless, this is nothing but a simple empirical analysis of the problem and more fundamental approaches are required to check its validity.

III. SUMMARY

We demonstrated that GGA is not sufficient for the description of the narrow t_{2g} band systems YTiO$_3$ and YVO$_3$. For example, it totally fails in predicting the stability of the magnetic structure of YVO$_3$ and overestimates the stability of the ground-state magnetic state of YTiO$_3$. The LDA+U method with the effective Coulomb interaction parameter U_{eff} chosen to reproduce the band gap can resolve most of the problems of GGA. The LDA+U method also describes

properly the correlation between the magnetic structure and small lattice distortion in two different phases of YVO$_3$.

For both YTiO$_3$ and YVO$_3$ the crystal structures obtained experimentally are assumed in the present calculations. For the e_g system LaMnO$_3$, GGA, and even LSDA can predict the ground-state magnetic structure properly for the experimental crystal structure.[1] However, the problem is not so simple. Once we optimize the crystal structure theoretically, GGA and even LDA+U cannot predict the ground state correctly. We have introduced an empirical corrections in the LDA+U method in order to solve this problem.

*Present address: Nippon Steel Corporation, Advanced Technology Research Laboratories, 3-35-1 Ida, Nakahara-ku, Kawasaki 211, Japan.

[1] N. Hamada, H. Sawada, and K. Terakura, in *Spectroscopy of Mott Insulators and Correlated Metals*, edited by A. Fujimori and Y. Tokura (Springer-Verlag, Berlin, 1995), p. 95.

[2] D. D. Sarma, N. Shanthi, S. R. Barman, N. Hamada, H. Sawada, and K. Terakura, Phys. Rev. Lett. **75**, 1126 (1995).

[3] I. Solovyev, N. Hamada, and K. Terakura, Phys. Rev. B **53**, 7158 (1996).

[4] H. Sawada, N. Hamada, K. Terakura, and T. Asada, Phys. Rev. B **53**, 12 742 (1996).

[5] I. Solovyev, N. Hamada, and K. Terakura, Phys. Rev. Lett. **76**, 4825 (1996).

[6] H. Sawada, Y. Morikawa, K. Terakura, and N. Hamada, Phys. Rev. B **56**, 12 154 (1997).

[7] J. P. Perdew, in *Electronic Structure of Solids 91*, edited by P. Ziesche and H. Eschrig (Akademie-Verlag, Berlin, 1991).

[8] J. P. Perdew, J. A. Chevary, S. H. Vosko, K. A. Jackson, M. R. Pederson, D. J. Smith, and C. Fiolhais, Phys. Rev. B **46**, 6671 (1992).

[9] V. I. Anisimov, J. Zaanen, and O. K. Andersen, Phys. Rev. B **44**, 943 (1991).

[10] I. V. Solovyev, P. H. Dederichs, and V. I. Anisimov, Phys. Rev. B **50**, 16 861 (1994).

[11] H. Sawada, N. Hamada, and K. Terakura, Physica B **237-238**, 46 (1997).

[12] There were some errors in the total energy calculations by the full-potential linearized augmented-plane-wave (FLAPW) method for YVO$_3$ in GGA in Ref. 4. The error was caused by the mixed use of different versions of GGA for different magnetic orderings. We have recalculated the total energies carefully by the FLAPW method with the cutoff energy of 12 Ry and 8 k points in the irreducible Brillouin zone based on the same ver-

sion of GGA as that used in the present calculation. Results of the total energies of YVO$_3$ for different magnetic orderings (G, C, A, and F) are 0.0 (G), -41.4 meV (C), -32.8 meV (A) and -36.7 meV (F). The total energy for the G-type AF was taken as the reference. These results are not yet totally consistent with those shown in Table II as E_T of GGA for YVO$_3$. We have confirmed a tendency that the higher cutoff energy makes the FLAPW results closer to the results in Table II. Note that the cutoff energy in the present pseudopotential calculation is 30.25 Ry, being much higher than that in the FLAPW calculation although the direct comparison is not necessarily meaningful. The number of sampling k points is also much larger in the present calculation.

[13] H. Kawano, H. Yoshizawa, and Y. Ueda, J. Phys. Soc. Jpn. **63**, 2857 (1994).

[14] P. Bordet, C. Chaillout, M. Marezio, Q. Huang, A. Santoro, S-W. Cheong, H. Takagi, C. S. Oglesby, and B. Batlogg, J. Solid State Chem. **106**, 253 (1993).

[15] T. Mizokawa and A. Fujimori, Phys. Rev. B **54**, 5368 (1996).

[16] D. Vanderbilt, Phys. Rev. B **41**, 7892 (1990).

[17] K. Laasonen, A. Pasquarello, R. Car, C. Lee, and D. Vanderbilt, Phys. Rev. B **47**, 10 142 (1993).

[18] N. Hamada (unpublished).

[19] D. A. Maclean, H.-N. Ng, and J. E. Greedan, J. Solid State Chem. **30**, 35 (1979).

[20] J. D. Garrett, J. E. Greedan, and D. A. Maclean, Mater. Res. Bull. **16**, 145 (1981).

[21] J. P. Goral, J. E. Greedan, and D. A. Maclean, J. Solid State Chem. **43**, 244 (1982).

[22] V. G. Zubkov, G. V. Bazuev, V. A. Perelyaev, and G. P. Shveikin, Fiz. Tverd. Tela (Leningrad) **15**, 1610 (1973) [Sov. Phys. Solid State **15**, 1079 (1973)].

[23] V. G. Zubkov, G. V. Bazuev, and G. P. Shveikin, Fiz. Tverd. Tela (Leningrad) **18**, 2002 (1976) [Sov. Phys. Solid State **18**, 1165 (1976)].